Journal of Materials Chemistry A

Accepted Manuscript

ROYAL SOCIETY OF CHEMISTRY

www.rsc.org/materialsA

The table of contents

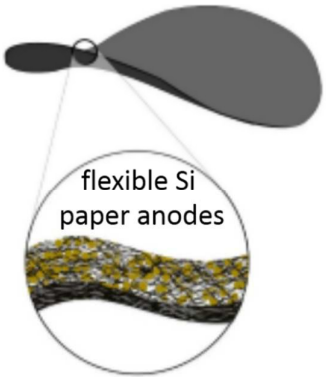

Rational design of high capacity, flexible Si paper anodes based on 3D conductive *Cladophora* nanocellulose matrix.

Cite this: DOI: 10.1039/c0xx00000x

www.rsc.org/xxxxxx

ARTICLE TYPE

Flexible Freestanding *Cladophora* Nanocellulose Paper based Si Anodes for Lithium-ion Batteries

Zhaohui Wang,*[a] Chao Xu,[a] Petter Tammela,[b] Jinxing Huo,[c] Maria Strømme,*[b] Kristina Edström,[a] Torbjörn Gustafsson[a] and Leif Nyholm*[a]

Received (in XXX, XXX) Xth XXXXXXXXX 20XX, Accepted Xth XXXXXXXXX 20XX
DOI: 10.1039/b000000x

Freestanding, lightweight and flexible Si paper anodes are prepared *via* a straightforward paper-making process using *Cladophora* nanocellulose, silicon nanoparticles and carbon nanotubes as the building blocks. The uniform Si particle distribution and strong adhesion of the Si nanoparticles to the porous, conductive and flexible nanocellulose/carbon nanotube 3D matrix yield specific capacities of up to 800 mAh g^{-1} (based on the weight of whole electrode) and very good cycling performances.

The development of lithium-ion batteries has constituted the foundation for the unprecedented advancement of portable electronic systems during the past two decades. To meet the needs of the next generation of flexible and sustainable electronic systems it is foreseen that significant efforts are necessary regarding the development of flexible, inexpensive and environmentally friendly lithium-ion batteries with high energy and power densities.[1, 2] Silicon has recently attracted extensive attention as an alternative anode material for lithium-ion batteries anodes owing to its high theoretical specific capacity (~ 4200 mAh g^{-1}) and abundance.[3-20] It is, however, well-known that silicon undergoes large volume changes upon lithiation and delithiation which results in pulverization of the anode and loss of contact between the silicon particles and the current collector which gives rise to rapid capacity fading.[4, 21, 22] Several routes have been explored to circumvent this problem including the incorporation of silicon particles into conducting coatings[23-25] as well as the development of silicon based nanostructures such as nanotubes,[26, 27] nanofibers[28, 29] and nanowires.[5, 30] Although promising capacities and improved cycling stabilities have been reported, the manufacturing of silicon based lightweight anodes with high mechanical strength and flexibility remains a challenge.

Currently, Si electrodes for lithium-ion batteries are usually manufactured by casting slurries containing silicon particles, conducting additives (such as carbon black) and polymeric binders onto metallic current collectors. The presence of the additives and the metallic current collector in particular, however, gives rise to a low mass fraction of the active material in the electrodes as well as extra manufacturing steps. This decreases the energy and power densities of the electrodes and also increases the cost of the lithium-ion batteries. More specifically, the silicon mass loading is normally 3~5 wt.% for a traditional Si electrode which corresponds to a capacity of only ~ 24 mAh g^{-1} when normalized with respect to the total mass of the electrode.[31] It is therefore clear that it should be possible to increase the energy and power densities of silicon based electrodes significantly by developing freestanding and binder-less electrodes. Significant efforts have so far been made to fabricate lightweight and self-standing silicon based electrodes by employing various types of carbon materials (e.g., graphene,[19, 31] and carbon nanotubes (CNT)[32, 33]) as additives in the manufacturing process. Lee et al.[19] developed a freestanding graphene/silicon anode by thermal reduction of a graphene oxide/silicon film while Ruoff et al.[31] prepared freestanding silicon anodes by casting a slurry of Si particles and polymer binder on a lightweight ultrathin-graphite foam. The latter electrodes exhibited a specific capacity of 983 mAh g^{-1} after normalization with respect to the weight of the electrode. Despite this development of freestanding silicon electrodes, reports on high capacity freestanding Si anodes with high mechanical flexibilities are still scarce.

In addition to the problems connected to the realization of high-performance silicon based anodes discussed above there are also important challenges concerning issues such as production time, cost and the possibilities of up-scaling the processes. Many of the so far developed freestanding silicon anodes contain graphene and specific CNTs (e.g. single-walled CNTs, ultralong CNTs and CNT sponges) which generally require precise synthetic control and therefore can be costly. High temperatures during several hours, or even days, are also often required in the post synthesis treatment processes. (see Supporting Information; **Table S1**) Economic and technical factors related to the possibilities of up-scaling the developed synthesis processes proposed for the making of Si anodes have unfortunately received very little attention in the literature so far. It is, nevertheless, clear that all the issues mentioned above need to be properly addressed in the development of inexpensive, flexible and sustainable energy storage systems with commercially viable specific energy and power densities and cycling stabilities.[34]

Advances in the development of flexible polymer and cellulose paper based energy storage devices,[2, 35-41] e.g. comprising conductive paper consisting of nanocellulose and carbon,[33, 35, 42-45] have recently provided new possibilities to address the challenges discussed above. It has been shown that cellulose may serve as a binder in the manufacturing of silicon

based electrodes for lithium-ion batteries,[46-48] although the latter electrodes were not flexible and freestanding due to the use of metallic substrates. Very recently, it was found that nanocellulose fibres can in fact constitute excellent building blocks in combination with CNTs to form strong and highly conductive networks suitable for flexible electronic applications.[33, 43, 49] Based on these findings it is reasonable to assume that paper-like, lightweight, freestanding and flexible Si anodes could be manufactured by incorporating silicon nanoparticles (SiNPs) into conductive CNT/nanocellulose matrices. We are, however, not aware of any reports on such flexible and freestanding SiNP/CNT/nanocellulose hybrid electrodes. Although previous reports on cellulose based paper-anodes/cathodes have been based on the use of cellulose fibres with micrometre diameters and/or nanofibrillated cellulose derived from wood pulp with low surface areas, crystallinities and high water contents,[37-39] these materials are not ideal in the manufacturing of high performance silicon based paper anodes since it is important to obtain a porous structure with a sufficiently high conductivity. As the latter should be possible to obtain by employing *Cladophora* nanocellulose it can be anticipated that this type of cellulose should be well-suited for the manufacturing of the desired flexible and freestanding Si paper anodes.

Herein, the manufacturing of a flexible, freestanding, lightweight silicon paper based anode is described for the first time based on a straightforward solution casting approach involving *Cladophora* nanocellulose fibres (CNC) and CNTs (see **Figure 1**). It is shown that the high surface area CNC[50] can serve as a dispersion agent and as flexible building blocks facilitating the attainment of a 3D porous structure and strong adhesion between the CNTs and SiNPs and that this approach gives rise to freestanding and flexible Si anodes for lithium-ion batteries. In contrast to the previously reported fabrication processes for freestanding silicon based anodes,[31, 51, 52] no post synthesis heat treatment and/or polymer binders are required to obtain a sufficiently high electrical conductivity and mechanical integrity of the electrodes. The as-synthesized anodes exhibit specific electrode capacities of ~ 800 mAh g^{-1} based on the weight of the electrodes, which corresponds to 3250 mAh g^{-1} based on the weight of the silicon particles at a current density of 0.2 A g^{-1}, and a specific electrode capacity of 458 mAh g^{-1} after 100 cycles at a current density of 1 A g^{-1}. As the presented method likewise can be utilized to fabricate lightweight and flexible, high-performance freestanding electrodes based on other active materials than silicon, the present approach clearly provides new possibilities for the manufacturing of flexible electrodes for a number of applications including portable electronics and medical devices.

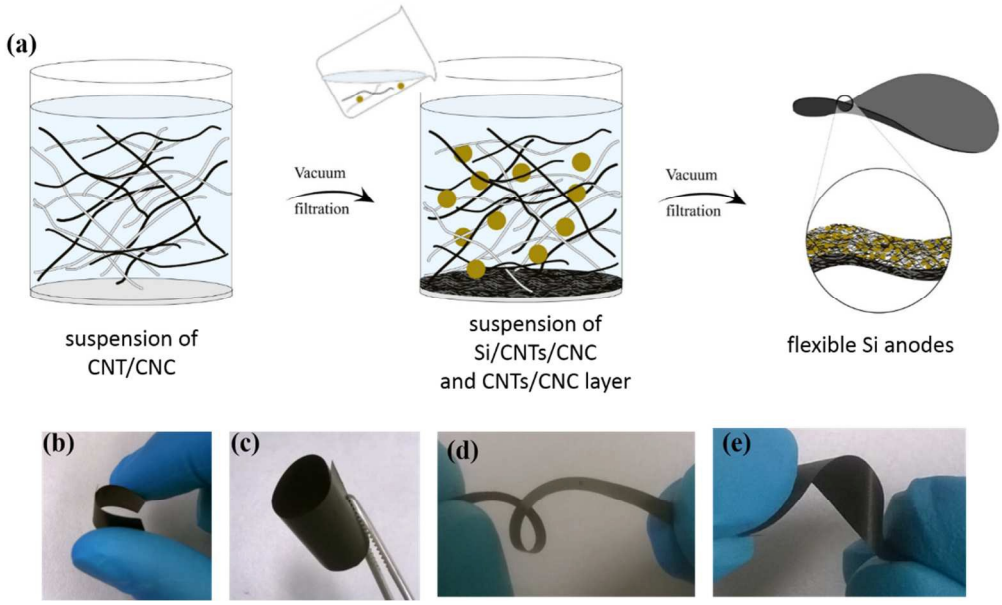

Figure 1. (a) Schematic illustration of the manufacturing process and the architecture of the obtained freestanding flexible Si-based composite anodes. Photographs of Si-based paper-like anodes under bending (b), rolling (c) and twisting (d and e).

As is illustrated in **Figure 1a**, the flexible and freestanding SiNP/CNT/CNC anodes are fabricated using a straightforward paper-making like process involving sequential vacuum filtration of water based dispersions containing the electrode components.[38, 39] The suspension of the CNC and CNTs was first sonicated to ensure good mixing after which the dispersion was vacuum-filtered through a filtering membrane until no liquid water was visible on the top of the membrane. A second dispersion, containing SiNPs, CNC and CNTs, was then vacuum filtered to generate a silicon containing layer on top of the supporting layer containing only CNC and CNTs. The ~30 µm thick paper-like and flexible freestanding SiNP/CNT/CNC electrode films were finally peeled off from the filter membrane (see the Experimental section in supporting information) and used as electrodes as is further described below. It should be pointed out that the incorporation of the SiNPs into the CNT/CNC network had almost no effect on the flexibility of the paper (see **Figures 1b-e**) and that the tensile strength and Young's modulus of the nanostructured SiNP/CNT/CNC paper were about 27.4 and 314 MPa (**Figure S1**), respectively. The as-obtained Si-based

anodes thus demonstrated excellent mechanical flexibility and could be bent, rolled and twisted without any resulting loss of performance (see **Figures 1b-e**).

The approach to fabricate flexible silicon based electrodes outlined in **Figure 1a** is expected to have several advantages with respect to current state-of-the art methods since: i) the CNC matrix serving as the composite backbone material provides the electrode with mechanical robustness and flexible paper-like properties;[35, 53] ii) the CNC acts both as an aqueous dispersion agent and binder which is expected to facilitate the attainment of a uniform distribution of CNTs and SiNPs as well as a good contact between the CNTs and SiNPs; iii) the CNT scaffold provides the required electron transport pathways while the CNC scaffold provides interconnected channels for effective ion transport[40, 45, 54]; iv) the interpenetrating flexible CNC and CNT network is expected to provide the mechanical robustness needed to withstand the volume expansion and contraction effects associated with the lithiation and delithiation of the SiNPs during the cycling; v) the bottom CNT/CNC network layer serves as a flexible substrate as well as a lightweight current collector; and finally vi) it should be possible to scale-up the manufacturing based on the industrial processes currently employed for paper making.[39]

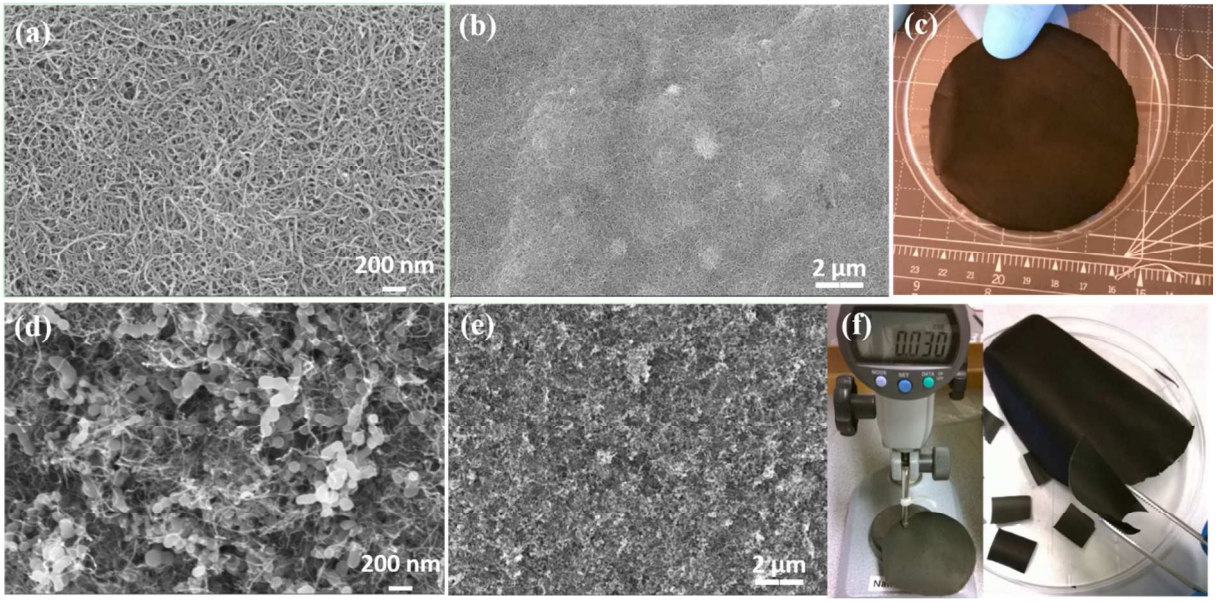

Figure 2 SEM images of the bottom CNT/CNC layer (a, b), the SiNP/CNT/CNC upper layer (d, e) and photographs of the CNT/CNC layer (c) and the SiNP/CNT/CNC layer (f), respectively.

As is demonstrated in the Supporting Information; **Figure S2**, the pristine CNC paper (not containing the CNFs and the Si particles) had a glossy white paper-like appearance while the SEM image revealed the presence of an open mesoporous structure in which the CNC fibres were randomly oriented. After the introduction of the CNTs, the structure of the obtained black and glossy composite was also porous with a flat surface as is seen in **Figures 2a-c**. Note that the conductivity of CNT/CNC composites matrix was measured to be ~15 S/cm (See **Figure S3**), indicating that the flexible and freestanding CNT/CNC paper can indeed be used as a conductive substrate in Si anode studied here. In **Figure 2b** it can further be seen that the entangled nanofibers created 3D interfibre voids with pore sizes of some tens of nanometres indicating that the structure of this composite was controlled by that of the CNC. If CNC was not added to the dispersed CNTs, a high agglomeration tendency for the CNTs was found which gave rise to a very rough and brittle material (see Supporting Information; **Figures S4a, b**). The latter clearly shows that the CNC served as an effective CNT dispersing agent. When the SiNPs were introduced into the CNT/CNC scaffold, the SiNPs appeared to become uniformly distributed within the porous nanostructure which consequently was retained as is evident from **Figures 2d and e**. In a composite containing only SiNPs and CNTs (i.e. and no CNC) the SiNPs were, on the other hand, found to agglomerate to form clusters (see Supporting Information; **Figures S5a and b**) and there was also an insufficient conductive wrapping of the SiNPs due to the formation of agglomerated CNTs, as seen from the light yellow area on the laminated black paper (Supporting Information; **Figure S5c**).

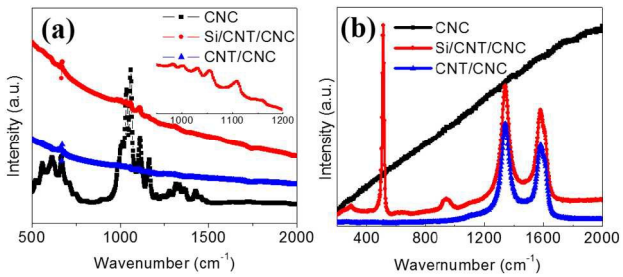

Figure 3 FTIR (a) and Raman (b) spectra for CNC, CNT/CNC and Si/CNT/CNC.

The diameters of the CNT and CNC used in our study were nearly the same, i.e. ~ 10 nm, and it is therefore difficult to distinguish between the CNT and the CNC in the SEM images particularly as the CNT and CNC are expected to be uniformly distributed. In order to further investigate the flexible Si/CNT/CNC anode, Raman and FTIR spectra were therefore carried out. The FTIR spectroscopy results for the CNC material show strong and well-defined peaks at 1113, 1057 and 1033 cm^{-1} in **Figure 3a**, the first being ascribed to the -OH glucose ring stretching and the two latter to C-OH stretching vibrations of cellulose..[53] Compared to the FTIR spectrum for the nanocellulose fibres, no peaks for Si and CNTs can be seen, while weak characteristic nanocellulose peaks also can be found in the Si/CNT/CNC paper electrode spectrum. The Raman spectrum from 200 to 2000 cm^{-1} is displayed in **Figure 3b**. No peaks were found for CNC. For the CNT/CNC material two strong peaks located at 1329 cm^{-1} and 1596 cm^{-1} were, however, observed, which can be assigned to a disorder band and the graphite band of carbon.[10] Compared to CNT/CNC, an additional peak was observed at 518 cm^{-1} for the Si/CNT/CNC material, due to the presence of crystalline Si nanoparticles.[27]

After cutting out pieces of the ~30 µm thick SiNP/CNT/CNC composite, see **Figure 2f**, these pieces were evaluated as freestanding lithium-ion battery anodes in polymer coated aluminium pouch (i.e. "coffee-bag") cells with metallic lithium foils as the counter electrodes. **Figure 4a** shows the 1st, 3rd and 5th cyclic voltammetry (CV) cycles for such a cell obtained at a scan rate of 0.1 mV s^{-1}. It is seen that a broad cathodic peak centred at 0.94 V vs. Li^+/Li and a small anodic peak at ~0.57 V vs. Li^+/Li was observed on the first cycle. As the peak at 0.94 V vs. Li^+/Li could not be seen on the subsequent cycles this peak most likely stemmed from the decomposition of the electrolyte yielding a solid electrolyte interface (SEI) layer on the high surface area electrode.[10, 55] The reduction peaks seen at ~0.18 V vs. Li^+/Li and at around the cut-off voltage of 0 V vs. Li^+/Li on the 3rd and 5th cycles can be ascribed to the formation of a lithium silicon alloy while the two oxidation peaks (located at ~0.38 V and ~0.58 V vs. Li^+/Li) appearing on the subsequent anodic scan stem from the oxidation of the alloy (i.e. the delithiation of amorphous Li_xSi to yield Si).[31] The fact that the current on the anodic scan increased with increasing cycle number can most likely be explained by a gradual activation of the SiNPs embedded in the conductive matrix as similar activation processes have been reported previously for Si-based anode materials.[24, 31, 55]

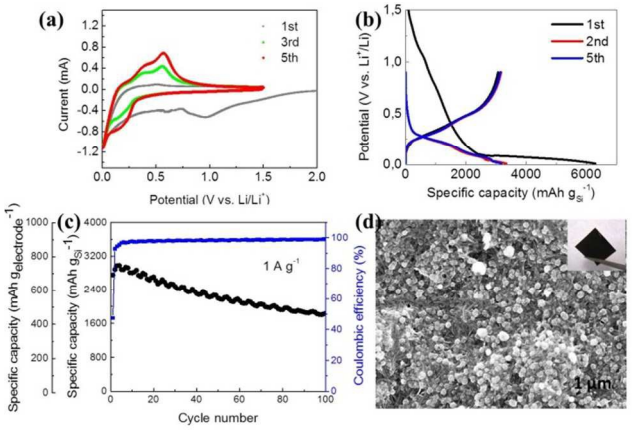

Figure 4 Electrochemical performance of the SiNP/CNT/CNC anodes showing 1st, 3rd and 5th cycle voltammograms (a) and 1st, 2nd and 5th cycle charge/discharge curves (b) as well as the corresponding specific capacity and coulombic efficiency vs. cycling number (c). SEM image of an anode after 100 charge/discharge cycles (d) with the inset showing a photograph of the anode.

The galvanostatic charge/discharge curves depicting the 1st, 2nd and 5th cycles obtained in a voltage window between ~ 0.01 and 1.0 V employing a current density of 1.0 A g^{-1} are shown in **Figure 4b**. On the 1st discharge cycle (i.e. reduction of the SiNP/CNT/CNC electrode) a continuous decrease in the potential from 1.5 to about 0.2 V vs. Li^+/Li and a pronounced voltage plateau at a potential slightly below 0.2 V Li^+/Li were seen which can be attributed to SEI formation and lithiation of crystalline Si to form amorphous Li_xSi, respectively, in good agreement with the cyclic voltammetry data. The first cycle charge and discharge capacities were found to be 6290 and 3070 mAh g^{-1} (based on the weight of the Si), respectively, corresponding to a coulombic efficiency (CE) of 49%. This value is similar to that of 43% found for PECVD prepared Si/CNT/Cellulose paper,[33] while CE values of 60~80% have been reported for Si-CNT freestanding electrode.[28, 51, 52, 55] It is therefore clear that low CE values constitute a general problem with cellulose and/or CNT based electrodes and that the CE values can vary somewhat depending on the electrode design (See **Table S2**).

The low coulombic efficiency for the first cycle, which also was observed for the CNT/CNC paper electrode (see **Figure S6a**), was most likely due to the irreversible formation of a SEI layer on the Si particles and the conductive CNT/CNC network as this has been frequently observed for other Si-CNT systems.[14, 28] The reduction of water, present in the CNC, and the reduction of the carboxylic groups of the CNT could, however, also contribute to the low initial CE value. In this context it should be pointed out that conducting polymer coatings have been reported to give improved performances.[14] The presence of at least one irreversible reduction reaction in the first charging cycle is supported by the fact that the coulombic efficiency was found to be higher than 95% in the second cycle. It should also be pointed out that the first cycle discharge capacity given above corresponds to a capacity of 766 mAh g^{-1} based on the full weight of the electrode. As the corresponding capacity of a CNT/CNC electrode was found to be 75 mAh g^{-1} (after normalization with respect to the electrode weight; see **Figure S6b**) it is evident that the CNT/CNC contribution to the capacity of the

SiNP/CNT/CNC electrode was less than 10 %. As is seen in **Figure 4b**, the second and fifth charge and discharge curves exhibited sloping voltage profiles rather than well-defined plateaus between 0.30 and 0.01 V, which can be explained by the lithiation and delithiation of amorphous silicon.[51]

Figure 4c presents the cycling performance of the SiNP/CNT/CNC anode containing cell in terms of the specific capacity as a function of the cycle number (obtained with a current density of 1 A g^{-1} and potential window between 0.01 and 1.0 V). While the capacity decreased gradually upon cycling, a capacity of 1840 mAh g^{-1} (based on the weight of the Si) was still obtained after 100 cycles. This value is significantly higher than those previously reported for many freestanding Si/C anodes cycled at lower current densities (i.e. Si/ multi-walled CNT paper (942 mAh g^{-1} after 30th cycle at 0.1 A g^{-1})[52] and (1450 mAh g^{-1} after 100th cycle at 0.4 A g^{-1})[31], 3D Si/C paper (1267 mAh g^{-1} after 100th cycle at 0.5 A g^{-1}),[51] as well as Si/CNT/PEDOT-Polystyrene sulfonate paper (1802 mAh g^{-1} after 100th cycle at 0.42 A g^{-1}),[55]). In addition, the capacity after 100 cycles was found to correspond to 67 % of the initial capacity for the Si/CNT/CNC anode. The latter should be compared with the corresponding values for a conventional Si electrode which exhibited a capacity of 623 mAh g^{-1} (based on the weight of the Si) and 51 % capacity retention after 80 cycles (see **Figure S7**). Since the lithiation and delithiation are associated with large volume change it is reasonable to ascribe the better cycling stability of the Si/CNT/CNC electrode to the flexibility and improved silicon attachment of the latter electrode. As is seen in the SEM image obtained for the Si/CNT/CNC electrode after 100 cycles (see **Figure 4d**), the SiNPs were still tightly embedded within the CNT/CNC networks. No cracks or disintegration of the Si/CNT/CNC paper anodes were observed indicating that the integrity of the Si/CNT/CNC paper electrode remained intact after the cycling.

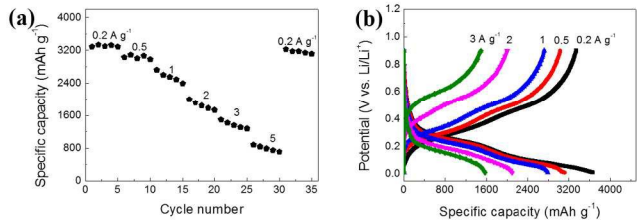

Figure 5 Rate capability of the flexible Si/CNT/CNC paper electrode. a) Specific capacity as a function of the cycle number for different current densities and b) charge and discharge curves for various current densities between 0.2 A g^{-1} and 3 A g^{-1}.

The Si/CNT/CNC paper anodes also showed good rate capabilities. **Figure 5a** shows the specific capacity of Si/CNT/CNC paper electrodes with a silicon loading of 0.78 mg cm^{-2} as a function of the cycle number for current densities ranging from 0.2 A g^{-1} to 5 A g^{-1}. The average capacity at a current density of 0.2 A g^{-1} was ~ 3250 mAh g^{-1} (based on the Si weight) which is approximately nine times higher that of commercial graphite anode materials (372 mAh g^{-1}). The capacity of the Si/CNT/CNC electrodes decreased with increasing current density, but a capacity of ~800 mAh g^{-1} (based on the Si weight) could still be obtained at a current density of 5 A g^{-1}. Furthermore, when the current density was changed back to 0.2 A g^{-1} after repeated cycling at different current densites, a specific capacity of 3200 mAh g^{-1} (based on the Si weight) was obtained. The latter value corresponds to a capacity of 800 mAh g^{-1} (based on the weight of the electrode) as well as an areal capacity of 2.5 mAh cm^{-2}. These values, are comparable or even higher than recently reported Si anodes in a similar system (see **Table S3**), particularly when considering the flexibility of the electrodes and the straightforward manufacturing process. In **Figure 5b,** which shows the charge/discharge curves obtained at different current densities, it is clearly seen that the shapes of the curves remained the same even at high rates. The latter clearly shows that the Si/CNT/CNC electrodes can undergo lithiation/delithiation even at high rates.

To summarize, we demonstrated that lightweight and flexible SiNP/CNT/CNC paper electrodes can be made with a straightforward paper-making approach which does not include any post-treatment processes. Owing to the uniform distribution and strong adhesion of the SiNPs to the 3D conductive flexible CNT/CNC network, these electrodes exhibit very promising energy storage performances, i.e., areal capacities of up to 2.5 mAh cm^{-2} and specific capacities of 3200 mAh g^{-1} (based on the weight of the Si) corresponding to electrode specific capacities of up to 800 mAh g^{-1} at 200 mA g^{-1}, as well as a capacity of 1840 mAh g^{-1} (based on the weight of the Si) after 100 cycles at a current density of 1 A g^{-1}. A flexible battery composed of a Si/CNT/CNC electrode and a lithium strip counter electrode was found to show similar capacities and charge/discharge curves for both the flat and the bent battery states (**Figure S8**). This indicates that the Si/CNT/CNC electrode is a viable alternative for flexible battery systems. The excellent electrochemical performance together with the straightforward industrially scalable preparation method hold great promise for the development of cost efficient, up-scalable and lightweight flexible high-energy anodes for lithium-ion batteries.

Acknowledgements

The Swedish Foundation for Strategic Research (SSF) (grant RMA-110012), The Swedish Energy Agency (project SwedGrids) and The Carl Trygger Foundation are gratefully acknowledged for financial support of this work.

Notes and references

[a] *Department of Chemistry-The Ångström Laboratory, Uppsala University, Box 538, SE-751 21 Uppsala, Sweden, E-mail: zhaohui.wang@kemi.uu.se leif.nyholm@kemi.uu.se;*
[b] *Nanotechnology and Functional Materials, Department of Engineering Sciences, The Ångström Laboratory, Uppsala University, Box 534, SE-751 21 Uppsala, Sweden, E-mail: maria.stromme@angstrom.uu.se;*
[c] *Applied Mechanics, Department of Engineering Sciences, The Ångström Laboratory, Uppsala University, Box 534, SE-751 21 Uppsala, Sweden.*

† Electronic Supplementary Information (ESI) available: [details of any supplementary information available should be included here]. See DOI: 10.1039/b000000x/

‡ Footnotes should appear here. These might include comments relevant to but not central to the matter under discussion, limited experimental and spectral data, and crystallographic data.

1. G. Zhou, F. Li and H.-M. h. Cheng, *Energy Environ. Sci.*, 2013, **7**, 1307.
2. Z. Wang, P. Tammela, P. Zhang, M. Strømme and L. Nyholm, *J. Mater. Chem. A*, 2014, **2**, 7711-7716.
3. H. Uono, B.-C. Kim, T. Fuse, M. Ue and J.-i. Yamaki, *J. Electrochem. Soc.*, 2006, **153**, A1708-A1708.
4. U. Kasavajjula, C. Wang and A. J. Appleby, *J. Power Sources*, 2007, **163**, 1003-1039.
5. C. K. Chan, H. Peng, G. Liu, K. McIlwrath, X. F. Zhang, R. A. Huggins and Y. Cui, *Nature Nanotech.*, 2008, **3**, 31-35.
6. L.-F. Cui, R. Ruffo, C. K. Chan, H. Peng and Y. Cui, *Nano lett.*, 2009, **9**, 491-495.
7. X. Chen, K. Gerasopoulos, J. Guo, A. Brown, C. Wang, R. Ghodssi and J. N. Culver, *ACS nano*, 2010, **4**, 5366-5372.
8. Y. J. Cho, H. S. Kim, H. Im, Y. Myung, G. B. Jung, C. W. Lee, J. Park, M. H. Park, J. Cho and H. S. Kang, *J Phys. Chem. C*, 2011.
9. H.-C. Tao, L.-Z. Fan, Y. Mei and X. Qu, *Electrochem. Commun.*, 2011, **13**, 1332-1335.
10. Z. Wang, X. Xiong, L. Qie and Y. Huang, *Electrochim. Acta*, 2013, **106**, 320-326.
11. Y. Yao, M. T. McDowell, I. Ryu, H. Wu, N. Liu, L. Hu, W. D. Nix and Y. Cui, *Nano Lett.*, 2011, **11**, 2949-2954.
12. S. R. Gowda, V. Pushparaj, S. Herle, G. Girishkumar, J. G. Gordon, H. Gullapalli, X. Zhan, P. M. Ajayan and A. L. M. Reddy, *Nano Lett.*, 2012, **12**, 6060-6065.
13. Y. Yao, N. Liu, M. T. McDowell, M. Pasta and Y. Cui, *Energy Environ. Sci.*, 2012, **5**, 7927-7930.
14. X. Su, Q. Wu, J. Li, X. Xiao, A. Lott, W. Lu, B. W. Sheldon and J. Wu, *Adv. Energy Mater.*, 2014, **4**, 1300882.
15. Q. Xiao, Q. Zhang, Y. Fan, X. Wang and R. A. Susantyoko, *Energy Environ. Sci.*, 2014, **7**, 2261-2268.
16. J.-Y. Choi, D. J. Lee, Y. M. Lee, Y.-G. Lee, K. M. Kim, J.-K. Park and K. Y. Cho, *Adv. Funct. Mater.*, 2012, **23**, 2108-2114.
17. B. P. N. Nguyen, N. A. Kumar, J. Gaubicher, F. Duclairoir, T. Brousse, O. Crosnier, L. Dubois, G. Bidan, D. Guyomard and B. Lestriez, *Adv. Energy Mater.*, 2013, **3**, 1351-1357.
18. M. Gauthier, D. Mazouzi, D. Reyter, B. Lestriez, P. Moreau, D. Guyomard and L. Roue, *Energy Environ. Sci.*, 2013, **6**, 2145-2155.
19. J. K. Lee, K. B. Smith, C. M. Hayner and H. H. Kung, *Chem. Commun.*, 2010, **46**, 2025-2027.
20. N. S. Hochgatterer, M. R. Schweiger, S. Koller, P. R. Raimann, T. Wöhrle, C. Wurm and M. Winter, *Electrochem. Solid-State Lett.*, 2008, **11**, A76-A80.
21. B. Liang, Y. Liu and Y. Xu, *J. Power Sources*, 2014, **267**, 469-490.
22. B. Philippe, R. Dedryvere, M. Gorgoi, H. Rensmo, D. Gonbeau and K. Edström, *J. Am. Chem. Soc.*, 2013, **135**, 9829-9842.
23. X. Chen, X. Li, F. Ding, W. Xu, J. Xiao, Y. Cao, P. Meduri, J. Liu, G. L. Graff and J.-G. Zhang, *Nano Lett.*, 2012, **12**, 4124-4130.
24. H. Wu, G. Yu, L. Pan, N. Liu, M. T. McDowell, Z. Bao and Y. Cui, *Nat. Commun.*, 2013, **4**, 1943.
25. J. W. Wang, X. H. Liu, K. Zhao, A. Palmer, E. Patten, D. Burton, S. X. Mao, Z. Suo and J. Y. Huang, *ACS Nano*, 2012, **6**, 9158-9167.
26. Z. Wen, G. Lu, S. Mao, H. Kim, S. Cui, K. Yu, X. Huang, P. T. Hurley, O. Mao and J. Chen, *Electrochem. Commun.*, 2013, **29**, 67-70.
27. M.-H. Park, M. G. Kim, J. Joo, K. Kim, J. Kim, S. Ahn, Y. Cui and J. Cho, *Nano lett.*, 2009, **9**, 3844-3847.
28. Q. Xiao, Y. Fan, X. Wang, R. A. Susantyoko and Q. Zhang, *Energy Environ. Sci.*, 2014, **7**, 655-661.
29. T. H. Hwang, Y. M. Lee, B.-S. Kong, J.-S. Seo and J. W. Choi, *Nano Lett.*, 2012, **12**, 802-807.
30. A. M. Chockla, K. C. Klavetter, C. B. Mullins and B. A. Korgel, *Chem. Mater.*, 2012, **24**, 3738-3745.
31. J. Ji, H. Ji, L. L. Zhang, X. Zhao, X. Bai, X. Fan, F. Zhang and R. S. Ruoff, *Adv. Mater.*, 2013, **25**, 4673-4677.
32. K. Evanoff, J. Benson, M. Schauer, I. Kovalenko, D. Lashmore, W. J. Ready and G. Yushin, *ACS nano*, 2012, **6**, 9837–9845.
33. L. Hu, N. Liu, M. Eskilsson, G. Zheng, J. McDonough, L. Wågberg and Y. Cui, *Nano Energy*, 2013, **2**, 138-145.
34. J. B. Goodenough, *Energy Environ. Sci.*, 2014, **7**, 14-18.
35. L. Nyholm, G. Nyström, A. Mihranyan and M. Strømme, *Adv. Mater.*, 2011, **23**, 3751-3769.
36. G. Nyström, A. Razaq, M. Strømme, L. Nyholm and A. Mihranyan, *Nano Lett.*, 2009, **9**, 3635-3639.
37. L. Jabbour, M. Destro, C. Gerbaldi, D. Chaussy, N. Penazzi and D. Beneventi, *J. Mater. Chem.*, 2012, **22**, 3227-3233.
38. S. Leijonmarck, A. Cornell, G. Lindbergh and L. Wågberg, *Nano Energy*, 2013, **2**, 794-800.
39. S. Leijonmarck, A. Cornell, G. Lindbergh and L. Wågberg, *J. Mater. Chem. A*, 2013, **1**, 4671-4677.
40. Z. Wang, P. Tammela, P. Zhang, J. Huo, F. Ericson, M. Strømme and L. Nyholm, *Nanoscale*, 2014, **6**, 13068-13075.
41. Z. Wang, C. Xu, P. Tammela, P. Zhang, K. Edström, T. Gustafsson, M. Strømme and L. Nyholm, *Energy Technology*, 2015, DOI: 10.1002/ente.201402224.
42. V. L. Pushparaj, M. M. Shaijumon, A. Kumar, S. Murugesan, L. Ci, R. Vajtai, R. J. Linhardt, O. Nalamasu and P. M. Ajayan, *Proc. Nati. Acad. Scie. U. S. A.*, 2007, **104**, 13574-13577.
43. M. Wang, I. V. Anoshkin, A. G. Nasibulin, J. T. Korhonen, J. Seitsonen, J. Pere, E. I. Kauppinen, R. H. Ras and O. Ikkala, *Adv. Mater.*, 2013, **25**, 2428-2432.
44. K.-H. Choi, S.-J. Cho, S.-J. Chun, J. T. Yoo, C. K. Lee, W. Kim, Q. Wu, S.-B. Park, D.-H. Choi, S.-Y. Lee and S.-Y. Lee, *Nano Lett.*, 2014, **14**, 5677-5686.
45. L. Hu, H. Wu, F. La Mantia, Y. Yang and Y. Cui, *ACS nano*, 2010, **4**, 5843-5848.
46. J. L. G. Cámer, J. Morales and L. Sánchez, *Electrochem. Solid-State Lett.*, 2008, **11**, A101-A104.
47. J. L. Gómez Cámer, J. Morales, L. Sánchez, P. Ruch, S. H. Ng, R. Kötz and P. Novák, *Electrochim. Acta*, 2009, **54**, 6713-6717.
48. S. S. Jeong, N. Böckenfeld, A. Balducci, M. Winter and S. Passerini, *J. Power Sources*, 2012, **199**, 331-335.
49. L. Jabbour, R. Bongiovanni, D. Chaussy, C. Gerbaldi and D. Beneventi, *Cellulose*, 2013, **20**, 1523-1545.
50. A. Mihranyan, A. P. Llagostera, R. Karmhag, M. Strømme and R. Ek, *Intern. J. Pharm.*, 2004, **269**, 433-442.
51. Y. Xu, Y. Zhu, F. Han, C. Luo and C. Wang, *Adv. Energy Mater.*, 2015, **5**, 1400753.

52. L. Yue, H. Zhong and L. Zhang, *Electrochim. Acta*, 2012, **76**, 326-332.
53. Z. Wang, P. Tammela, M. Strømme and L. Nyholm, *Nanoscale*, 2015, **7**, 3418-3423.
54. D. O. Carlsson, A. Mihranyan, M. Strømme and L. Nyholm, *RSC Adv.*, 2014, **4**, 8489-8497.
55. Z. Chen, J. W. F. To, C. Wang, Z. Lu, N. Liu, A. Chortos, L. Pan, F. Wei, Y. Cui and Z. Bao, *Adv Energy Mater*, 2014, **4**, 1400207.